Journal of Power Sources 448 (2020) 227445

Contents lists available at ScienceDirect

Journal of Power Sources

journal homepage: www.elsevier.com/locate/jpowsour

Pre-blended conductive agent to effectively improve the storage properties of $LiNi_{0.6}Co_{0.2}Mn_{0.2}O_2$ cathode materials

Xiangbang Kong, Shiyun Peng, Jiyang Li, Zhenjie Chen, Zhiqiang Chen, Jing Wang, Jinbao Zhao *

State-Province Joint Engineering Laboratory of Power Source Technology for New Energy Vehicle, Engineering Research Center of Electrochemical Technology, Ministry of Education, College of Chemistry and Chemical Engineering, Xiamen University, Xiamen, 361005, PR China

HIGHLIGHTS

- Greatly improve the storage performance of the high-nickel ternary material.
- Do not introduce unnecessary substances, and maintain the advantage of high capacity.
- Inhibit the increase in alkalinity of the material surface during storage.
- Simple and effective, with the potential for large-scale applications.

ARTICLE INFO

Keywords:
Lithium-ion battery
$LiNi_{0.6}Co_{0.2}Mn_{0.2}O_2$
Cathode
Storage properties

ABSTRACT

Nowadays, the high-nickel ternary cathode materials attract more and more attention because of their high capacity. However, compared with other cathode materials, the disadvantage of high-nickel ternary cathode materials in storage performance is very obvious. The obvious impurities on the surface of high-nickel ternary materials are generated after storage for a period of time, and its electrochemical performance produce a cliff-like decline. In this work, we use the pre-blending of conductive agent to simply and effectively improve the storage performance of $LiNi_{0.6}Co_{0.2}Mn_{0.2}O_2$ cathode materials under high temperature and high humidity conditions. Fine particles of conductive agent can be well filled in the gap between the primary particles of the material, suppressing the sites where impurities are most easily formed during storage. Compared with the pristine materials, when stored for the same time, the impurities generated on the surface of modified materials are significantly fewer, the increase of weight is smaller, and more excellent electrochemical performance is exhibited. It can be seen from the results that the pre-blending of the conductive agent can greatly improve the storage performance of the high-nickel ternary cathode materials.

1. Introduction

In recent years, the $LiNi_xCo_yMn_{1-x-y}O_2$ (NCM) materials have received widespread attention because of their high specific capacity, high power density, and relatively low price [1–3]. Since the NCM cathode materials can provide a specific capacity higher than 170 $mAh{\cdot}g^{-1}$ when the Ni content is more than 60%, it is one of the most popular cathode materials on the market. However, as the Ni content in the NCM materials increases, the thermal stability, cycle stability, and storage stability in the air will all decrease [4–7]. Currently, the NCM333 and NCM523 materials have been successfully commercialized and applied to some power batteries. The $LiNi_{0.6}Co_{0.2}Mn_{0.2}O_2$ (NCM622) has a higher specific capacity, and is being gradually promoted and applied now. As mentioned before, many NCM materials with higher nickel content have problems of poor storage performance [8–11], and the NCM622 materials are no exception. When the content of Ni^{3+} in the material is higher, the material will be more unstable and be more susceptible to air, which will bring an increase in mass [12]. The degradation mechanism of $LiNiO_2$-based materials in air is the transition from Ni^{3+} to Ni^{2+}, accompanied by the extraction of lattice lithium and lattice oxygen evolution [13].

When the $LiNi_xCo_yMn_{1-x-y}O_2$ materials are stored in air for a certain period of time, the significant LiOH and Li_2CO_3 impurities will generate on the surface of materials, and will cause severe performance

* Corresponding author.
E-mail address: jbzhao@xmu.edu.cn (J. Zhao).

https://doi.org/10.1016/j.jpowsour.2019.227445
Received 8 August 2019; Received in revised form 3 November 2019; Accepted 10 November 2019
Available online 17 November 2019
0378-7753/

degradation [14,15]. For example, when the materials are stored for some time, the generated impurities will cause the surface lattice Li to escape, resulting in an increase in the spacing of the transition metal layers [16]. The structure of the material is thus destroyed [17–21], and the impedance of the material is going to significantly increase [22], and so is the polarization of the electrode [23]. So far, researchers have made some attempts to enhance the storage performance of $LiNi_xCo_yMn_{1-x-y}O_2$ materials. For example, Liu et al. coated a layer of $LiCoO_2$ on the surface of NCA, and the storage performance in the air under room temperature is obviously improved [24]. Zhang et al. coated Li_2MnO_3 on the surface of $LiNi_{0.8}Co_{0.1}Mn_{0.1}O_2$, which made smaller amount of impurities formed on the surface after kept in the air for two months, and the electrochemical performance was greatly improved [25]. Zheng et al. rinsed the NCM811 with ethanol, and after storage for 40 days in air, the surface-generated Li_2CO_3 impurities were significantly reduced [26]. However, these work still have problems such as complicated process and introduction of impurities, and it is difficult to achieve large-scale application. In order to meet the needs of actual production, it is necessary to develop a simple and effective method to improve the storage performance of high-nickel ternary cathode materials. At the same time, through previous studies [14,22], it is known that during the storage of the high-nickel ternary cathode materials, the pores and junctions of the primary particles on the surface preferentially react with the moisture, carbon dioxide and other components in the air to form adsorbing substances or impurities. Therefore, inhibiting the growth of impurities between primary particle gaps may play an important role in improving the storage performance of ternary cathode materials.

In this work, the conductive agents are mixed with NCM622 materials in advance, taking the advantage of fine particle size of the conductive agent to fill the gap among the primary particles of the NCM622 materials, and reducing the formation of impurities on the surface of the NCM622 materials. This method is simple and easy to implement, and has been shown to effectively inhibit degradation of NCM622 materials during storage.

2. Experimental section

2.1. Preparation and storage of materials

The pristine NCM622 materials used in the experiment were provided by Beijing Easpring Material Technology Co., Ltd. (China). The modification of the material was mainly carried out by the following steps: firstly, the positive electrode materials (NCM622) and the conductive agent (acetylene black, AB) were ball-milled and blended with the weight ratio of 8 : 1. In this process, the conductive agent was embedded in the primary particle gap of the positive electrode material. Then the mixture was calcined in an Ar atmosphere after blending to enhance the bonding force between NCM622 and AB.

After the preparation of the materials, the pristine materials and the modified materials were respectively subjected to high temperature and high humidity storage experiments. During the experiment, 4 copies of two materials, each about 5 g, were put in 55 °C, 80% RH (relative humidity) constant temperature and humidity oven. The four materials were stored for 1–4 weeks, and the stored materials were taken out weekly for physical and electrochemical performance tests.

2.2. Electrochemical tests

The batteries used for the tests were assembled as follows. For the pristine NCM622 materials before and after storage, 80 wt% of NCM622 material, 10 wt% of acetylene black, and 10 wt% of PVDF (polyvinylidene fluoride) were uniformly mixed and dissolved in NMP (N-methyl-1,2-pyrrolidne) solvent to prepare a slurry. For the modified materials before and after storage, since acetylene black of one-eighth of the mass of the positive electrode materials had been added in the modification process, only one-ninth of PVDF of the total mass of the modified materials needed to be added in the process of preparing the slurry. After the slurry was evenly mixed, it was uniformly coated on the surface of the aluminum foil current collector, and stored in an oven at 80 °C for 24 h to evaporate the solvent. The mass loading of active material of positive electrodes was 6–8 mg cm^{-2}. The prepared positive electrodes and the negative electrodes of Li were assembled into the 2016 coin-cells, the separator was provided by Asahi Kasei, and the electrolyte was LB-301 electrolyte (1 M $LiPF_6$ in EC/DMC, ethyl cellulose/dimethyl carbonate, 1 : 1 m/m), provided by Zhangjiagang Guotai-Huarong New Chemical Materials Co., Ltd. The charge and discharge process were carried out at a current density of 16 mA g^{-1} at a constant current and constant voltage of 3.0–4.3 V.

2.3. Physical characterization

After the storage experiments were completed, a chemical titration method was used to detect the alkali content of the surface of the materials after storage. During the test, the material of 1 g is dissolved in deionized water of 100 ml and stirred for 5 min in a sealed environment, and filtered to obtain a clear liquid. The titration is carried out again using the calibrated hydrochloric acid. The SEM (Scanning electron microscopy, S-4800, Hitachi Corporation) was used to observe the topographical changes of the surface of the material before and after

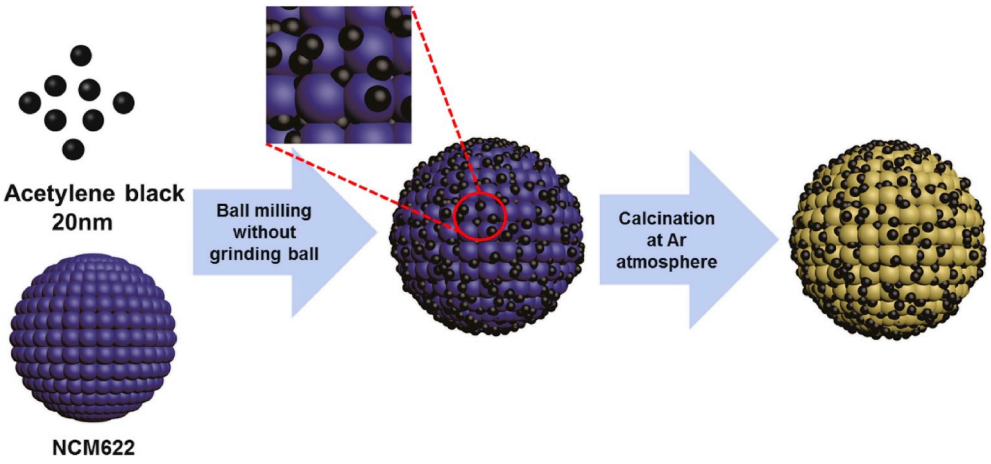

Fig. 1. Schematic diagram of the experiment.

storage. TEM (Transmission electron microscope, Tecnai F30) was used to observe the impurities generated on the surface of the material. The Raman spectroscopy (Raman spectrometer, Renishaw RT 1000) was used to detect the formation of impurities on the surface of the material after storage. The XRD (X-ray diffraction, Rigaku IV) was used to study the change of material structure during storage.

3. Results and discussion

3.1. Storage performance analysis

The schematic diagram of the process of this experiment is shown in the Fig. 1. In the experiment, the conductive agent with fine particle size is embedded in the gap of the primary particles of NCM622 materials during the blending process due to the friction between each other. Also, the bonding force between the conductive agent and the NCM 622 particles can be increased by using a calcination method in an inert atmosphere. At the same time, by conducting an FTIR analysis test on the conductive agent acetylene black materials (Fig. S1), it can be clearly seen that there are obvious acidic groups such as hydroxyl groups and carboxyl groups in the acetylene black materials, and the presence of these acidic components is beneficial to inhibit the alkalinity of NCM622 materials to some extent during the experiment.

During the experiment, the time of blending between acetylene black and NCM622 materials and the calcination temperature of the mixed materials will have an important influence on the experimental results. Hence, the best conditions of the experiment have been explored. As shown in the Fig. S2, at the speed of 500 rpm, the samples are blended for 1 h, 2 h, 3 h and 4 h, respectively. From the comparison of experimental results, it can be clearly seen that when the blending time reaches 4 h or 8 h, the cycle performance and rate performance of the positive electrode materials are significantly reduced, which may be due to the long time of blending, resulting in the materials rupture during the excessively long blending process. When the blending time is one or 2 h, the electrochemical performance of the materials is almost the same with the control sample. And it can be seen from the Fig. S3 that the conductive agent particles can be uniformly mixed with the NCM622 materials after blending for one or 2 h, and therefore, for the simplicity of the experiment, the blending time of 1 h has been selected as the experimental protocol.

The calcination temperature during the experiment also affects the experimental results, and the 400 °C, 500 °C and 600 °C have been

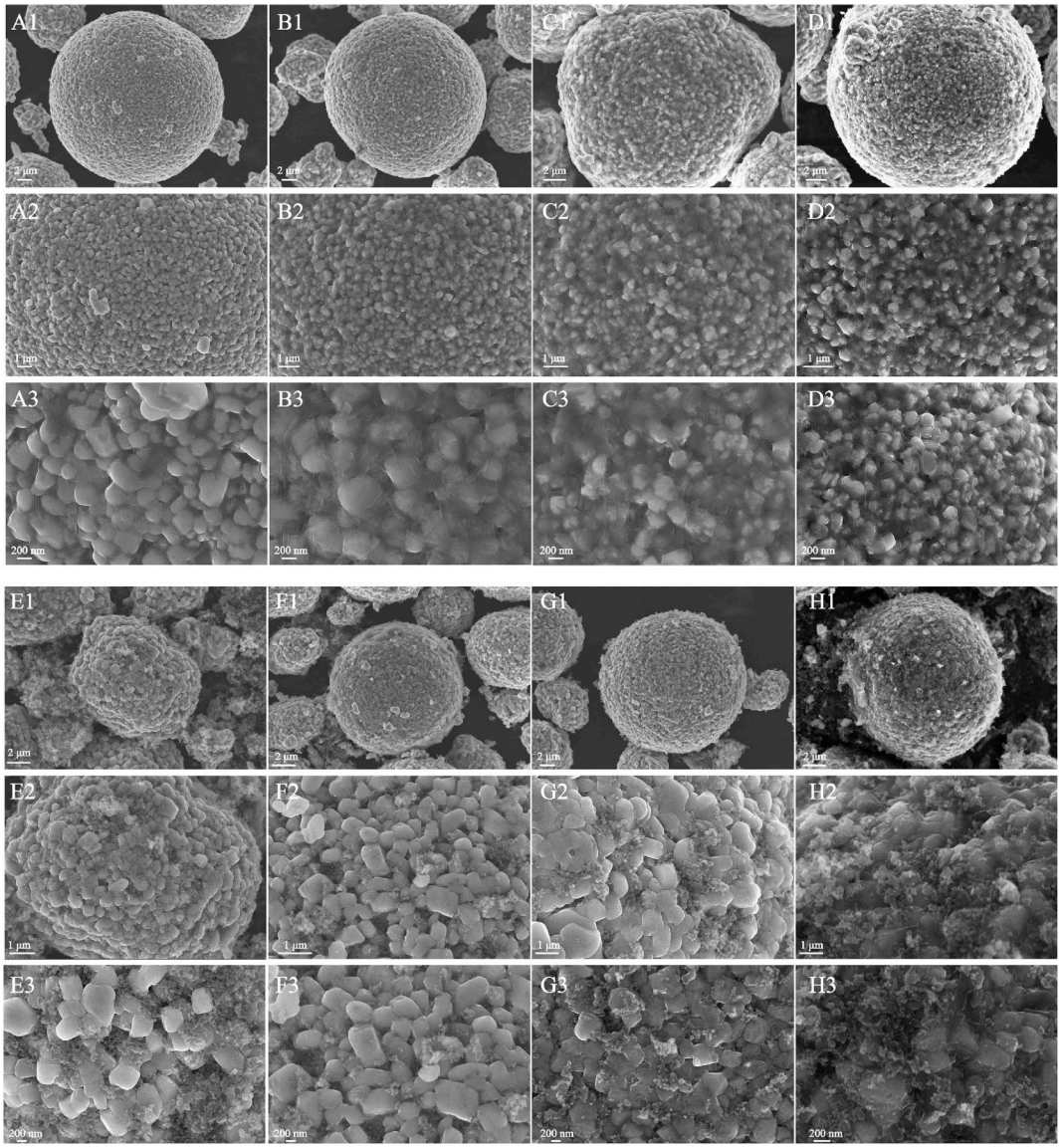

Fig. 2. SEM images of NCM622 and NCM622-AB materials after storage for 1–4 weeks. A1 ~ A3: NCM622-1 week, B1 ~ B3: NCM622-2 weeks, C1 ~ C3: NCM622-3 weeks, D1 ~ D3: NCM622-4 weeks, E1 ~ E3: NCM622-AB-1 week, F1 ~ F3: NCM622-AB-2 weeks, G1 ~ G3: NCM622-AB-3 weeks, H1 ~ H3: NCM622-AB-4 weeks.

selected to explore the suitable calcination temperature. The XRD test results of the calcined materials are shown in the Fig. S4. At calcination temperatures of 400 °C and 500 °C, the NCM622 materials still maintain a good layered structure. However, when the calcination temperature reaches 600 °C, the characteristic (018)/(110) splitting diffraction peak of NCM622 is no longer obvious, which indicates that at the temperature of 600 °C, the structure of the materials is destroyed. In addition, the diffraction peaks of Li_2CO_3, metal and metal oxide phases appear in the XRD pattern of the material. This is probably because acetylene black has a relatively high activity at a high temperature of 600 °C, and the $LiNi_{0.6}Co_{0.2}Mn_{0.2}O_2$ materials are reduced to form the above substances. In addition, ultrasonication was performed separately on materials calcined at 400 °C and 500 °C. Same mass of materials were dissolved in the same volume of deionized water and sonicated for 5 min in an ultrasonic device with a frequency of 40 kHz. It can be seen from the experimental results (Fig. S5) that after ultrasonication, acetylene black particles were partly separated from the NCM622-AB-400 °C materials and floated in the upper layer of the solution, while NCM622-AB-500 °C material showed no obvious separation of acetylene black particles. Thus, indicating that the binding force of NCM622 and acetylene black material is indeed stronger under the calcination conditions of 500 °C. Therefore, in order to maintain the structure of the NCM622 materials, and to increase the bonding force of the acetylene black and the NCM622 materials as much as possible, 500 °C is chosen as the final

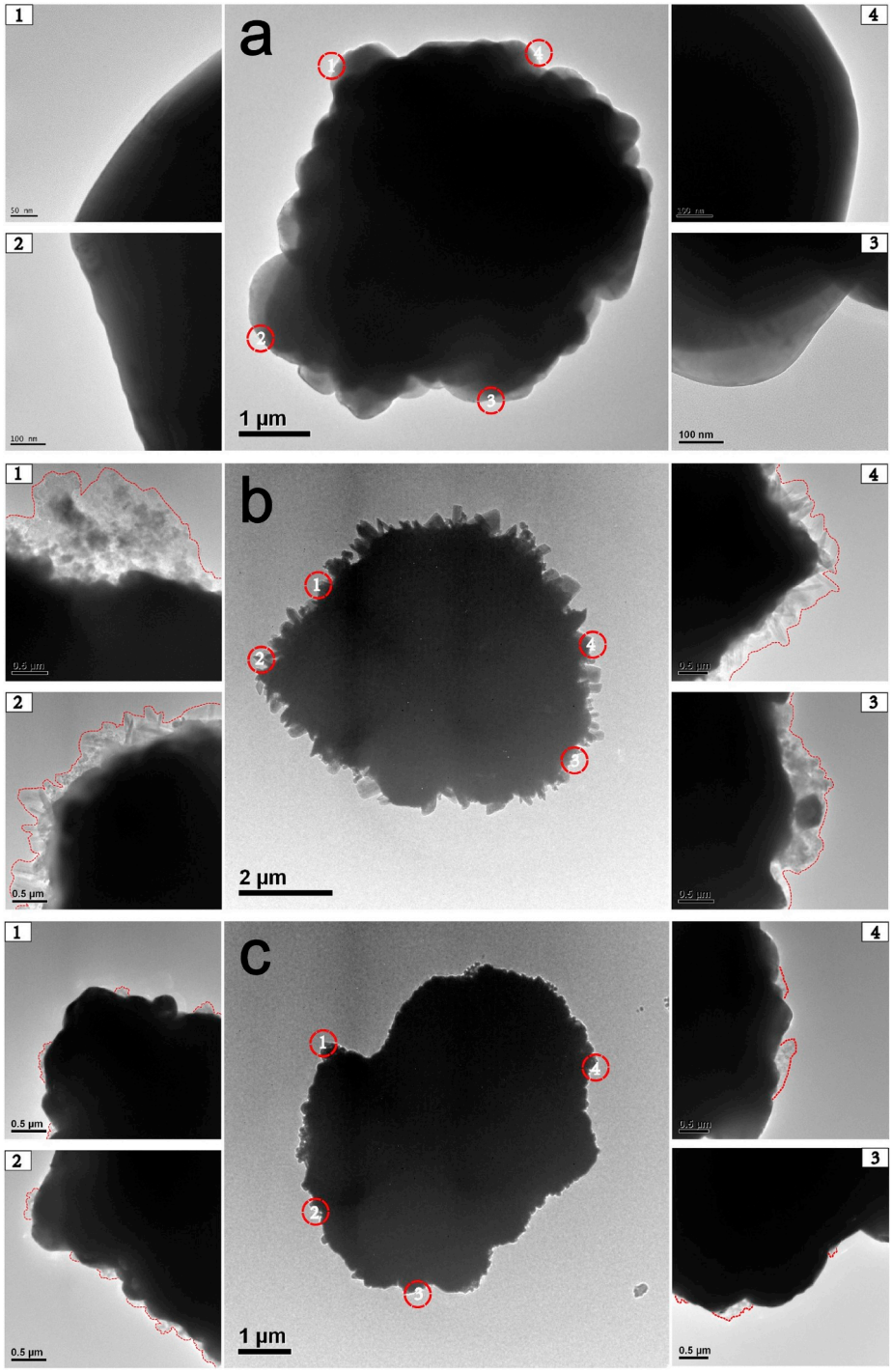

Fig. 3. TEM images of pristine NCM622, NCM622-4 weeks and NCM622-AB-4 weeks materials. a: pristine NCM622, b: NCM622-4 weeks, c: NCM622-AB-4 weeks.

calcination temperature. The final materials produced are written as NCM622-AB.

In order to investigate the storage properties of the materials before and after modification, the original NCM622 materials and NCM622-AB materials have been stored in a constant temperature and humidity chamber of 55 °C and 80% RH from one to four weeks. And two copies of materials have been taken out to calculate the weight increasing rate every other week. From the experimental results (Fig. S6), it can be clearly seen that the mass gain rate of the modified materials NCM622-AB is significantly lower than that of the original NCM622 materials after storage for the same time. For the original materials, the mass gain rate is 1.6966% after storage of 1 week, and the mass gain rate reaches 4.1717% after storage of 4 weeks. For the modified materials, the mass gain rate is only 0.5967% after storage of 1 week, and is just 1.3786% after storage of 4 weeks. In addition, according to the literature [7], it is known that the mass gain rate of ternary cathode materials during storage is proportional to the 1/2 power of storage time. The NCM622 and NCM622-AB materials also conform to this rule. It can be clearly seen that the slope of the curve corresponding to NCM622-AB is smaller, which also indicates that it has better storage performance.

So as to more intuitively compare the changes in surface topography of the two materials after storage for the same time, the SEM tests have been performed on the two materials before and after storage. The Fig. 2 is a comparison of the morphology of NCM622 and NCM622-AB materials stored at 55 °C, 80% RH for one to four weeks. Compared with pristine NCM622 materials (Fig. S7A1-A3). It can be clearly seen from the Fig. 2 that after storage of 1 week (Fig. 2A1-A3), the significant impurities have been formed in the gaps between the primary particles of the NCM622 materials. After 4 weeks of storage (Fig. 2D1-D3), the surface is covered with flaky impurities, and some of the primary particles are completely covered. The longer the storage time, the more impurities are generated. From the Fig. 2E and F, it is obvious that for the modified materials, after storage for one and two weeks, since the primary particle gap is filled with acetylene black, almost no impurities are formed on the surface. And as the storage time increases (Fig. 2G and H), the impurities appear slowly on the surface of the materials, but the amount of impurities generated is significantly lower than that of the original materials, which is consistent with the results of previous weight increasing rate. In addition, TEM tests were also performed on the pristine NCM622 material, NCM622-4 weeks and NCM622-AB-4 weeks materials. In the test, four sites of each sample were randomly selected for magnification observation. From the test results (Fig. 3), it can be seen that the surface of original NCM622 materials is smooth and no impurity exists on the surface. After the storage for 4 weeks, in the

Table 1
First cycle charge and discharge performance of NCM622 and NCM622-AB materials.

Samples	First cycle discharge specific capacity ($mAh \cdot g^{-1}$)	First cycle efficiency (%)
NCM622-pristine	162.19	81.77
NCM622-1 week	130.91	72.56
NCM622-2 weeks	78.80	48.06
NCM622-3 weeks	65.93	40.95
NCM622-4 weeks	50.57	32.24
NCM622-AB-1 week	154.32	79.17
NCM622-AB-2 weeks	151.79	79.08
NCM622-AB-3 weeks	149.83	75.99
NCM622-AB-4 weeks	141.82	73.64

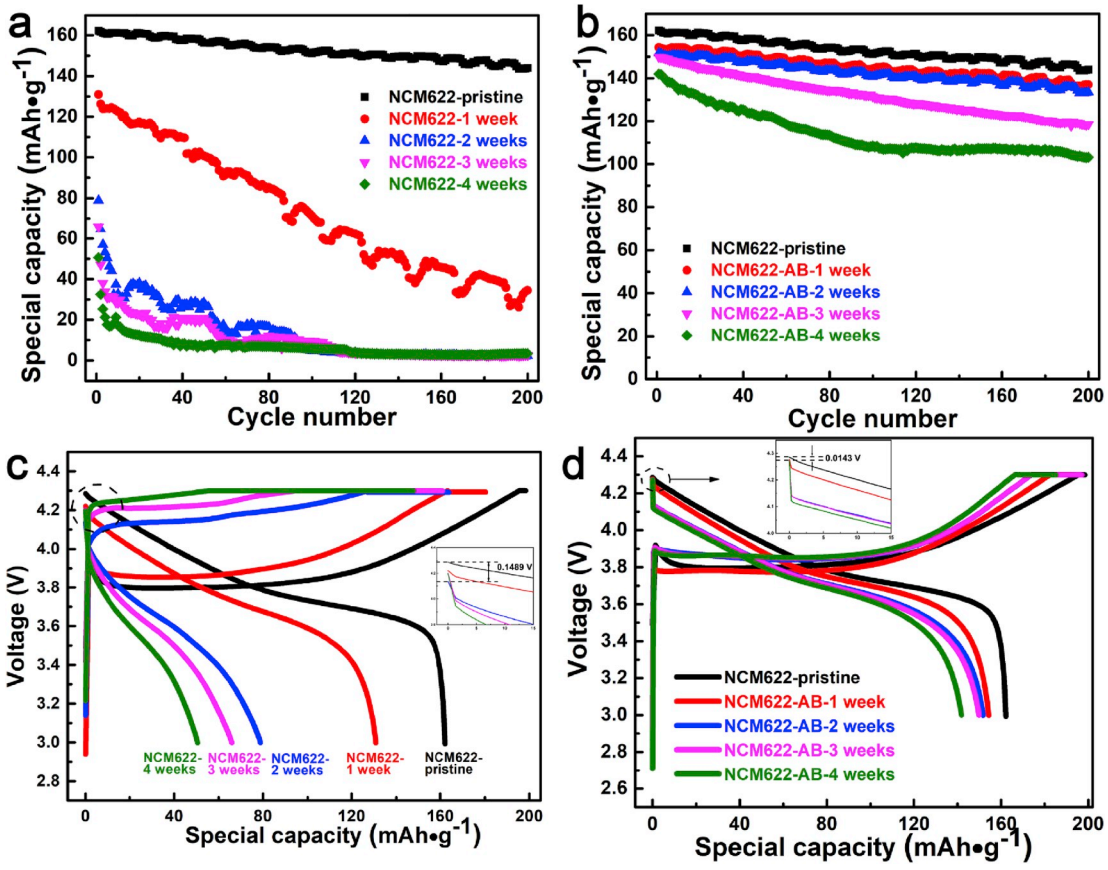

Fig. 4. Electrochemical performance of NCM622 and NCM622-AB materials after storage for 1–4 weeks. Cycle performance of storage: (a) NCM622 and (b) NCM622-AB; First charge and discharge curves of (c) NCM622 and (d) NCM622-AB.

TEM characterization, a large amount of impurities form on the surface of NCM622 materials, and the generated impurities almost completely wrap the NCM622 materials. At the same time, from the partial enlarged view, the average thickness of the generated impurity layer reaches about 500 nm. For the NCM622-AB material, after 4 weeks of storage, sporadic and discontinuous impurities appear on only a few parts of the surface, and the thickness of the impurities is much smaller than that of the NCM622 material. The results of the TEM test are in good agreement with the SEM test results.

3.2. Electrochemical performance

After the storage experiment, the materials obtained have been tested for the electrochemical performance. The test results are shown in the Fig. 4. The Fig. 4a and b show the electrochemical test results of the modified and pristine NCM622 materials after storage for one to four weeks, respectively. It can be clearly seen from the figures that after the modification, there is a significant improvement on the electrochemical cycle performance of the NCM622-AB materials after storage. For the NCM622 materials, after storage of one week under high temperature and high humidity situations, the cycle performance is significantly reduced, and after storage of 2–4 weeks, its electrochemical performance presents a cliff-like decline, followed by the discharge capacity fading rapidly to around zero. However, for the NCM622-AB materials, it still maintains good cycle performance after storage of 1–2 weeks, and its performance is reduced to a small extent after storage of 4 weeks, but it is still much better than the NCM622 materials. The Fig. 4c–d shows the results of the first cycle charge and discharge test of NCM622 and NCM622-AB materials after storage for 1–4 weeks. In addition, the electrochemical cycle coulombic efficiency of the material after storage is shown in Fig. S8. It can be clearly seen from the figure that the coulombic efficiency of the original materials during the cycle is lower and the fluctuation is more pronounced than that of the NCM622-AB materials. The specific results are shown in the Table 1. From the table it can be clearly seen that the unmodified materials, as the storage time increases, the efficiency of charge and discharge in the first cycle is continuously reduced, and the specific capacity of the first cycle is also greatly reduced. After storage of 4 weeks, the charge and discharge efficiency of the material is drastically reduced from the original 81.77%–32.24%, and the discharge specific capacity of the material is sharply reduced from the original 162.19 mAh·g^{-1} to 50.57 mAh·g^{-1}. However, the reduction rate of the first charge and discharge efficiency of the modified material is much smaller, and the specific discharge capacity of the first cycle is only reduced from 162.19 mAh·g^{-1} of the original material to 141.82 mAh·g^{-1}. There is a noticeable improvement compared with the unmodified material.

At the same time, through the Fig. 4c-d, it can be observed that in the comparison of the charge and discharge voltage drop in the first cycle of the battery, the first cycle discharge voltage drop of NCM622 materials after storage of 4 weeks is 0.1489 V, and the voltage drop of NCM622-AB is only 0.0143 V. This is mainly because the adsorbed substances and impurities formed on the surface of the stored materials have low ion/electron conductivity, and some active particles are isolated during charge and discharge, resulting in a decrease in the capacity of the material and the initial discharge voltage [14,23].

In order to analyze why the initial discharge voltage drops during the charging and discharging process, different materials have been tested for the AC impedance. The test results are shown in the Fig. 5. In the EIS spectrum, at 4.30 V, the materials before and after storage all have three semicircles corresponding to the impedance of lithium ions passing through the SEI (solid electrolyte interphase) membrane, the impedance of electron transfer, and the charge transfer impedance, respectively

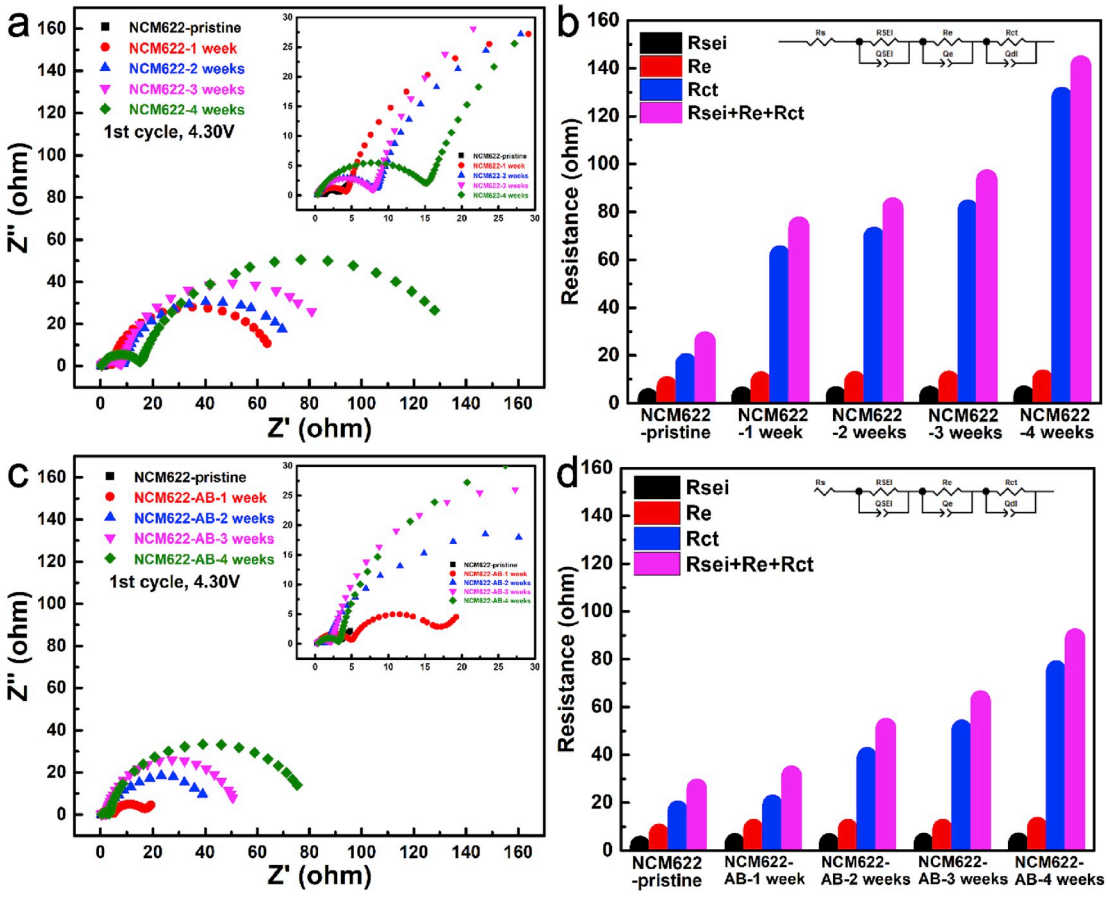

Fig. 5. AC impedance maps of NCM622 and NCM622-AB after storage for 1–4 weeks.

[27–29]. By comparing the impedance values of the two materials after storage for one to four weeks, it is found that the impedance of the cell assembled with NCM622 materials is significantly greater than that of the NCM622-AB materials. And in the impedance analysis, there is no significant change in the SEI film impedance and electron transfer impedance, but the charge transfer impedance of NCM622 materials after storage is greatly increased (the detailed impedance values are shown in the Table S1). It is generally believed that the charge transfer impedance is caused by an electrochemical reaction at the interface between the materials and the electrolyte accompanied by charge exchange. In the positive electrode materials of a lithium ion battery, the charge transfer is caused by the valence state change of transition metals M (Ni, Co, and Mn) and the entry of Li^+ into the materials. Therefore, the increase in charge transfer resistance of the stored materials may be caused by poor conductors of ions/electrons on the surface of the stored materials. This is in good agreement with the previous SEM test and electrochemical performance test results.

Further, the materials have been assembled into the batteries for the cyclic voltammetry test after storage for different durations, and the test results are shown in the Fig. 6. Before and after storage, an oxidation peak and a reduction peak appear respectively, representing the extraction and embedding of lithium ions [30,31], and there is no new redox peak appeared in the cycle interval. At the same time, it can be seen that the oxidation peak shifts to a higher potential with the extension of the storage time, and the reduction peak shifts to a lower potential. It shows that the storage time has a great influence on the reduction and oxidation peak of the first cycle of the materials. It is mainly because the materials will react with the composition of the electrolyte when contacting with the electrolyte, and form poor conductors of ions/electrons covering the surface of the material, resulting in an increase in electrode polarization and a large difference in the peak of the oxidation and reduction. As can be seen from the Fig. 6a, for the NCM622 materials, after storage of one week, the oxidation peak is clearly shifted to a higher potential, and as the storage time increases, the degree of the offset increases. Although the NCM622-AB materials also have a similar potential shift, the degree is significantly lighter (Fig. 6b). In addition, by comparing the CV test results of NCM622 and NCM622-AB materials after the same storage time (Fig. 6c–d), it can be seen that the degree of redox peak shift of NCM622 materials is significantly greater than that of NCM622-AB materials, which also proves that the storage performance of NCM622-AB material has been significantly improved.

3.3. Physical characterization

In the previous section, we have studied the changes in the storage performance of the materials before and after modification and their electrochemical properties, but the research on the properties of the materials itself is not sufficient. Therefore, the physical properties of the materials itself have been explored to further explain the reasons for the performance improvement.

As shown in the Fig. 7, the Raman spectroscopy tests have been performed on the materials after storage. In the Raman test, the peaks around 600 cm^{-1} and 500 cm^{-1} are assigned to the A_{1g} and E_g vibration modes of the NCM622 materials, respectively. The A_{1g} vibration mode is a symmetric stretching vibration mode of M − O (M represents a transition metal atom). In this vibration mode, two O atoms adjacent to the M atoms are symmetrically stretched and vibrated parallel to the c-axis. The Eg vibration mode belongs to the O-*M*-O, and the bending vibration mode is sequentially perpendicular to the c-axis [32–34]. The absorption peak at 1093 cm^{-1} is attributed to the resonance absorption of Li_2CO_3[32]. The Fig. 7a–b and Fig. 7c–d shows the Raman test results of NCM622 original materials and NCM622-AB materials, respectively, after storage for different durations. From the test results in the figure, it can be clearly seen that the intensity of Li_2CO_3 peak of NCM622-AB materials after storage is significantly lower than that of NCM622 materials. This indicates that the content of impurities formed on the surface of the modified material after storage is significantly lower, which is in good agreement with the experimental results of mass gain in the foregoing. At the same time, it is well known that the presence of impurities such as Li_2CO_3 on the surface significantly increases the surface alkalinity of the ternary material, thereby further affecting its overall performance. To

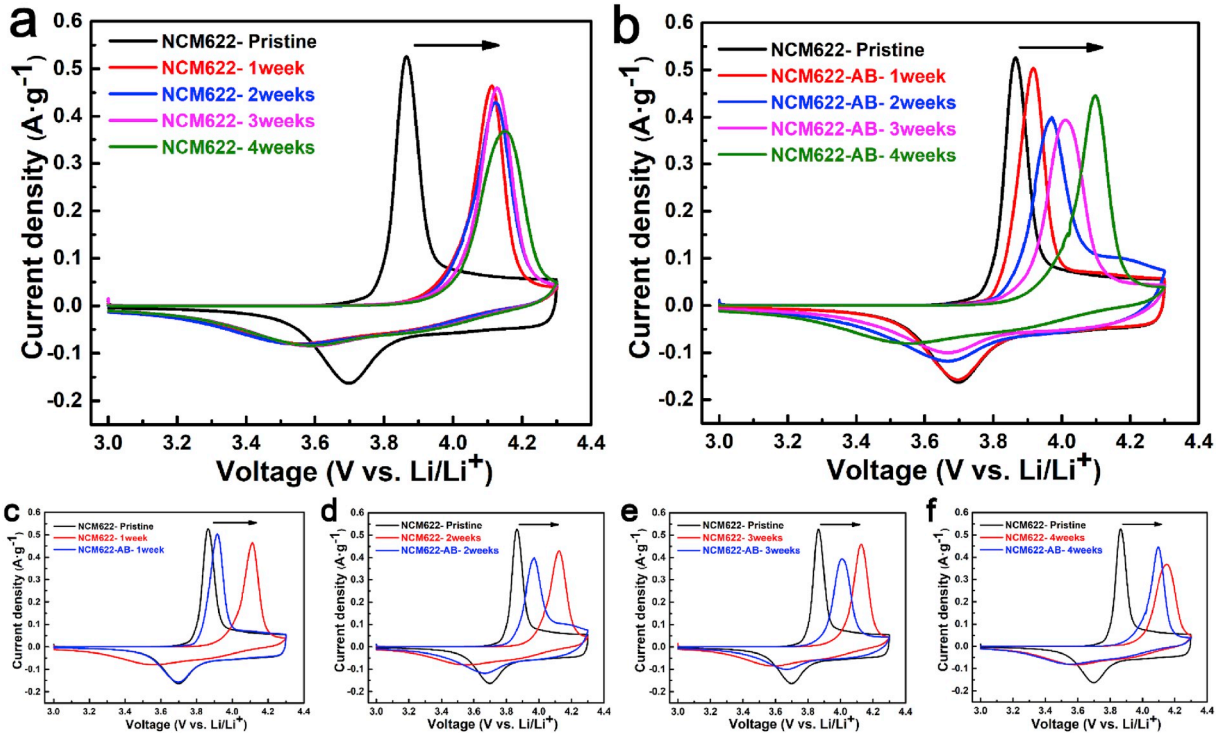

Fig. 6. The first cycle CV test chart of NCM622 and NCM622-AB materials after storage for different time.

this end, the surface alkali content of the two materials stored after 1–4 weeks has been tested by the chemical titration. Since the alkaline component of the surface impurities is mainly a lithium salt, the test results (Fig. S9) are shown by the mass fraction of Li contained in the impurities per gram of material. It can be found from the test results that the surface alkalinity of the NCM622 materials is much higher than that of the NCM622-AB materials under the same storage conditions, which is also consistent with the peak intensity difference of Li_2CO_3 in the Raman test. Meanwhile, the Raman test results of the two materials at the same storage time have been compared (Fig. S10). It can be seen from the comparison results that the intensity ratio of A_{1g}/E_g of NCM622 material (Table S2) is significantly lower than that of NCM622-AB material (Table S3) under the same storage time. According to the literature, it is known that in the initial stage of charging, the intensity of the A_{1g} vibration mode of $LiMO_2$ is rapidly attenuated, while the E_g vibration mode remains stable, and the intensity ratio of A_{1g}/E_g drops rapidly. This is mainly due to the release of lithium, which causes the local v (MO_6) mode to be affected. The A_{1g} vibration mode reacts more directly to this effect, and the E_g mode is less affected [35]. The intensity ratio of A_{1g}/E_g of NCM622 material after storage is significantly lower, which indicates that more Li is eluted from the NCM622 materials during the storage process, thereby generating more Li_2CO_3, and causing more serious damage and performance degradation.

On the other hand, in order to more precisely study the structural changes of the materials after storage, the materials after storage have been subjected to XRD tests. And in order to more accurately describe the change of the peak position of the materials before and after storage, 10 wt% natural graphite is added to the materials, and evenly mixed and tested. The diffraction peak of the NCM622 materials is corrected based on the peak of graphite at 26.54°. As shown in the Fig. 8, the crystal structures of the materials after storage are not changed, and the characteristic peaks such as (003) and (104) indicate that the materials before and after storage have a typical space group structure of R-3m of α-NaFeO2 type [32,36]. A partial enlarged view of the (003) crystal plane is shown in the Fig. 8c–d. As the storage time increases, the diffraction peaks of the (003) crystal plane will shift toward the low Bragg angle, and the longer the storage time, the larger the angle of the offset. It is generally believed that the (003) crystal plane diffraction peak represents diffraction of X-rays by two adjacent transition metal layers. In the in-situ XRD test, in the initial stage of charging (delithiation), the elution of Li leads to an increase in the electrostatic repulsion of the adjacent O layer, an increase in the interlayer spacing, and finally an increase in the pitch of the transition metal layer, causing the (003) crystal plane diffraction peak to shift to a low Bragg angle [17–21]. During the storage process, the formation of the impurity Li_2CO_3 will cause the surface lattice Li to escape, resulting in an increase in the transition metal layer spacing [16]. It can be clearly seen from the Fig. 8c–d that the offset of the (003) crystal plane of the NCM622-AB material is lower than that of the NCM622 material under the same storage time. Therefore, the XRD test results also show that the amount of Li released by the NCM622-AB material during storage is less, which is consistent with the previous Raman test results.

4. Conclusions

In this work, the pre-blending conductive agent acetylene black is

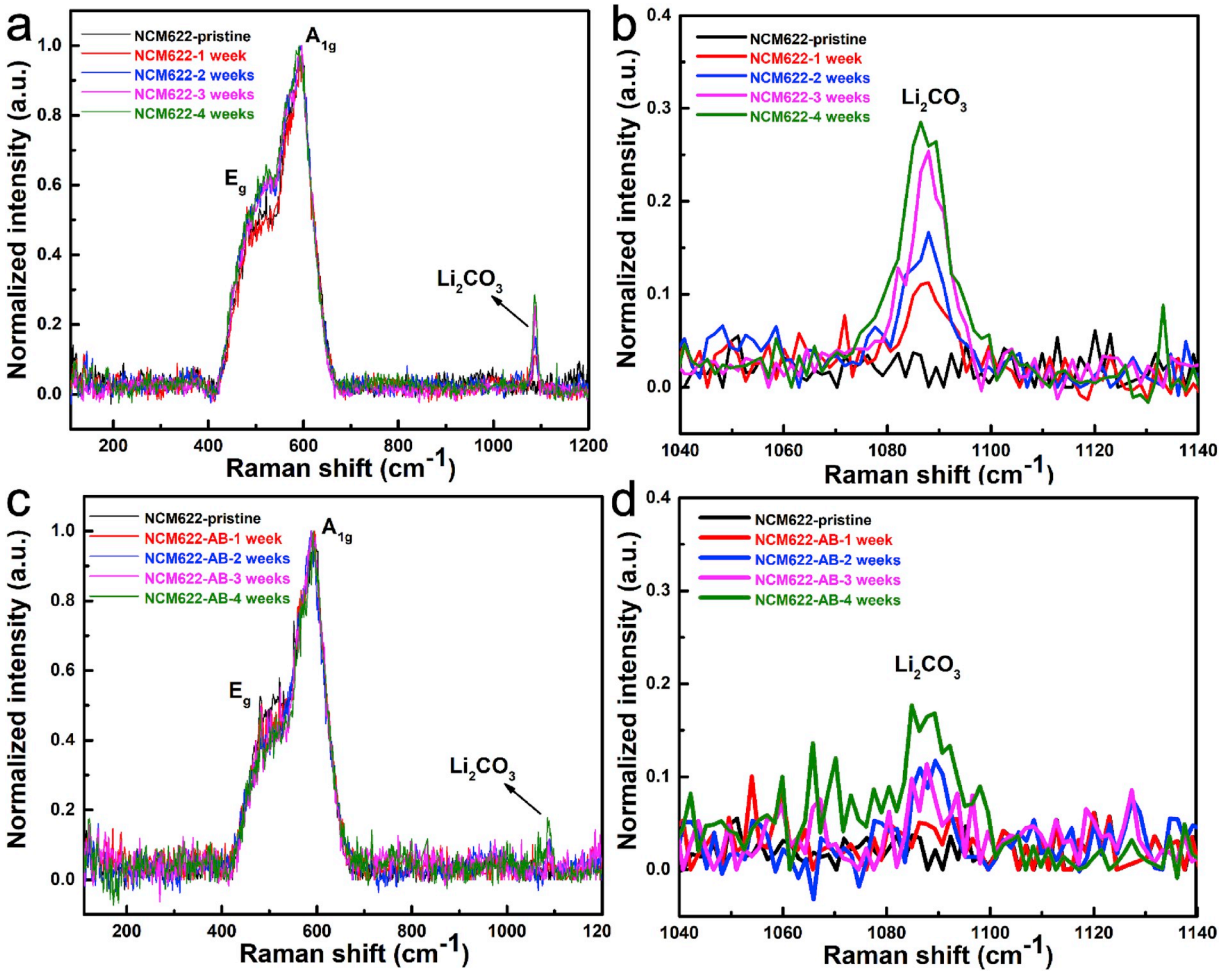

Fig. 7. Raman test results for NCM622 and NCM622-AB materials after storage for different time.

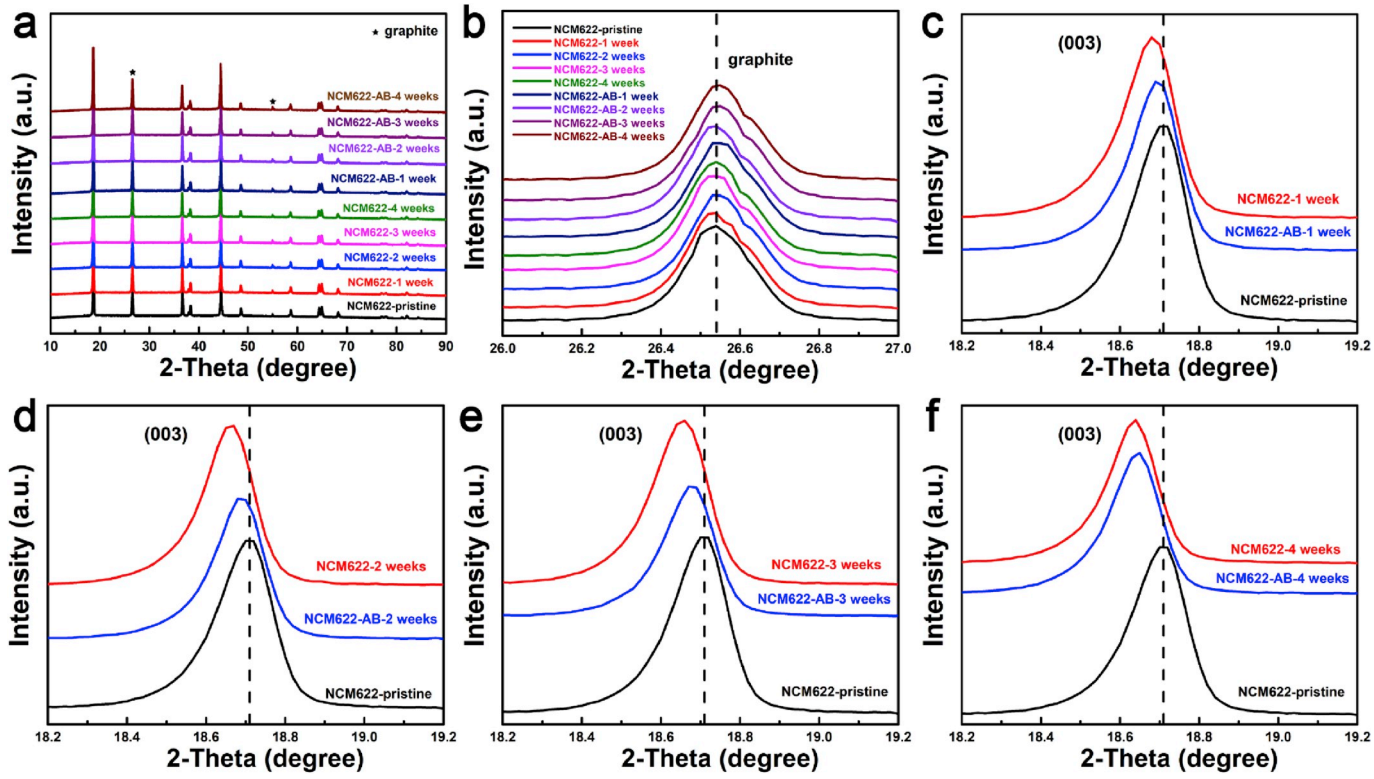

Fig. 8. XRD test results for NCM622 and NCM622-AB materials after storage for different time.

used to embed into the pores and joints of primary particles on the surface of the NCM622 material to form an embedded composite structural material, thereby reducing the adsorption of gas at the pores, and slowing the formation of adsorbate materials and impurities. This method can greatly improve the storage performance of $LiNi_{0.6}Co_{0.2}Mn_{0.2}O_2$ cathode material. Moreover, the acidic group of the conductive agent acetylene black itself can inhibit the surface alkalinity of the material to some extent during the blending process. Since the conductive agent is indispensable in the process of preparing the electrodes, this method will not introduce unnecessary substances, will not reduce high-capacity advantage of $LiNi_{0.6}Co_{0.2}Mn_{0.2}O_2$ cathode materials and have the advantage of simplicity and effectiveness. Therefore, the method has a good application prospect.

Declaration of competing interests

The authors declare that they have no known competing financial interests or personal relationships that could have appeared to influence the work reported in this paper.

Acknowledgements

We gratefully acknowledge the financial support of National Key Research and Development Program of China (2017YFB0102000), National Natural Science Foundation of China (21603179,21621091), the Fundamental Research Funds for the Central Universities (20720170021). The authors also thank Prof. Daiwei Liao for his valuable suggestions.

Appendix A. Supplementary data

Supplementary data to this article can be found online at https://doi.org/10.1016/j.jpowsour.2019.227445.

References

[1] S.M. Bak, et al., Structural changes and thermal stability of charged LiNixMnyCozO (2) cathode materials studied by combined in situ time-resolved XRD and mass spectroscopy, ACS Appl. Mater. Interfaces 6 (2014) 22594–22601, https://doi.org/10.1021/am506712c.
[2] Y. Bi, et al., Correlation of oxygen non-stoichiometry to the instabilities and electrochemical performance of LiNi0.8Co0.1Mn0.1O2 utilized in lithium ion battery, J. Power Sources 283 (2015) 211–218, https://doi.org/10.1016/j.jpowsour.2015.02.095.
[3] A. Manthiram, J.C. Knight, S.-T. Myung, S.-M. Oh, Y.-K. Sun, Nickel-Rich and lithium-rich layered oxide cathodes: progress and perspectives, Adv. Energy. Mater. 6 (2016), 1501010, https://doi.org/10.1002/aenm.201501010.
[4] H.-J. Noh, S. Youn, C.S. Yoon, Y.-K. Sun, Comparison of the structural and electrochemical properties of layered Li[NixCoyMnz]O2 (x = 1/3, 0.5, 0.6, 0.7, 0.8 and 0.85) cathode material for lithium-ion batteries, J. Power Sources 233 (2013) 121–130, https://doi.org/10.1016/j.jpowsour.2013.01.063.
[5] L. Ma, M. Nie, J. Xia, J.R. Dahn, A systematic study on the reactivity of different grades of charged Li[NixMnyCoz]O2 with electrolyte at elevated temperatures using accelerating rate calorimetry, J. Power Sources 327 (2016) 145–150, https://doi.org/10.1016/j.jpowsour.2016.07.039.
[6] J. Li, J.M. Zheng, Y. Yang, Studies on storage characteristics of LiNi0.4Co0.2Mn0.4O2 as cathode materials in lithium-ion batteries, J. Electrochem. Soc. 154 (2007) A427–A432, https://doi.org/10.1149/1.2711068.
[7] K. Matsumoto, R. Kuzuo, K. Takey, A. Yamanaka, Effects of CO2 in air on Li deintercalation from LiNi1−x−yCoxAlyO2, J. Power Sources 81–82 (1999) 558–561.
[8] H. Liu, Y. Yang, J. Zhang, Investigation and improvement on the storage property of LiNi0.8Co0.2O2 as a cathode material for lithium-ion batteries, J. Power Sources 162 (2006) 644–650, https://doi.org/10.1016/j.jpowsour.2006.07.028.
[9] W. Liu, G. Hu, K. Du, Z. Peng, Y. Cao, Enhanced storage property of LiNi0.8Co0.15Al0.05O2 coated with LiCoO2, J. Power Sources 230 (2013) 201–206, https://doi.org/10.1016/j.jpowsour.2012.12.065.
[10] G.V. Zhuang, et al., Li2CO3 in LiNi0.8Co0.15Al0.05O2 cathodes and its effects on capacity and power, J. Power Sources 134 (2004) 293–297, https://doi.org/10.1016/j.jpowsour.2004.02.030.
[11] D.-H. Cho, et al., Effect of residual lithium compounds on layer Ni-rich Li [Ni0.7Mn0.3]O2, J. Electrochem. Soc. 161 (2014) A920–A926, https://doi.org/10.1149/2.042406jes.
[12] K. Shizuka, C. Kiyohara, K. Shima, Y. Takeda, Effect of CO2 on layered Li1+zNi1−x−yCoxMyO2 (M=Al, Mn) cathode materials for lithium ion batteries, J. Power Sources 166 (2007) 233–238, https://doi.org/10.1016/j.jpowsour.2007.01.013.

[13] H.S. Liu, Z.R. Zhang, Z.L. Gong, Y. Yang, Origin of deterioration for LiNiO2 cathode material during storage in air, Electrochem. Solid State Lett. 7 (2004) A190, https://doi.org/10.1149/1.1738471.
[14] Z. Chen, et al., The high-temperature and high-humidity storage behaviors and electrochemical degradation mechanism of LiNi0.6Co0.2Mn0.2O2 cathode material for lithium ion batteries, J. Power Sources 363 (2017) 168–176, https://doi.org/10.1016/j.jpowsour.2017.07.087.
[15] J. Eom, M.G. Kim, Cho, J. Storage Characteristics of LiNi[sub 0.8]Co[sub 0.1+x]Mn[sub 0.1−x]O[sub 2] (x=0, 0.03, and 0.06) Cathode Materials for Lithium Batteries, J. Electrochem. Soc. 155 (2008) A239, https://doi.org/10.1149/1.2830946.
[16] C. Villevieille, P. Lanz, C. Bünzli, P. Novák, Bulk and surface analyses of ageing of a 5V-NCM positive electrode material for lithium-ion batteries, J. Mater. Chem. 2 (2014) 6488, https://doi.org/10.1039/c3ta13112b.
[17] J.N. Reimers, J.R. Dahn, Electrochemical and in situ X-ray diffraction studies of lithium intercalation in LixCoO2, J. Electrochem. Soc. 139 (1992) 2091–2097, https://doi.org/10.1149/1.2221184.
[18] W. Li, J.N. Reimers, J.R. Dahn, In situ x-ray diffraction and electrochemical studies of Li1−xNiO2, Solid State Ion. 67 (1993) 123–130.
[19] M. Balasubramanian, X. Sun, X.Q. Yang, J. McBreen, In situ X-ray diffraction and X-ray absorption studies of high-rate lithium-ion batteries, J. Power Sources 92 (2001) 1–8.
[20] Xiao-Qing Yang, J. McBreen, W.-S. Yoon, C.P. Grey, Crystal structure changes of LiMn0.5Ni0.5O2 cathode materials during charge and discharge studied by synchrotron based in situ XRD, Electrochem. Commun. 4 (2002) 649–954.
[21] O. Dolotko, A. Senyshyn, M.J. Mühlbauer, K. Nikolowski, H. Ehrenberg, Understanding structural changes in NMC Li-ion cells by in situ neutron diffraction, J. Power Sources 255 (2014) 197–203, https://doi.org/10.1016/j.jpowsour.2014.01.010.
[22] Z. Chen, et al., Electrochemical degradation mechanism and thermal behaviors of the stored LiNi0.5Co0.2Mn0.3O2 cathode materials, ACS Appl. Mater. Interfaces 10 (2018) 25454–25464, https://doi.org/10.1021/acsami.8b07873.
[23] P. Oh, B. Song, W. Li, A. Manthiram, Overcoming the chemical instability on exposure to air of Ni-rich layered oxide cathodes by coating with spinel LiMn1.9Al0.1O4, J. Mater. Chem. 4 (2016) 5839–5841, https://doi.org/10.1039/c6ta01061j.
[24] W. Liu, et al., Synthesis and characterization of LiCoO2-coated LiNi0.8Co0.15Al0.05O2 cathode materials, Mater. Lett. 83 (2012) 11–13, https://doi.org/10.1016/j.matlet.2012.05.100.
[25] H. Zhang, et al., Effects of Li2MnO3 coating on the high-voltage electrochemical performance and stability of Ni-rich layer cathode materials for lithium-ion batteries, RSC Adv. 6 (2016) 22625–22632, https://doi.org/10.1039/c5ra26897d.
[26] X. Zheng, et al., Investigation and improvement on the electrochemical performance and storage characteristics of LiNiO 2 -based materials for lithium ion battery, Electrochim. Acta 191 (2016) 832–840, https://doi.org/10.1016/j.electacta.2016.01.142.
[27] Q.-C. Zhuang, et al., An electrochemical impedance spectroscopic study of the electronic and ionic transport properties of spinel LiMn2O4, J. Phys. Chem. C 114 (2010) 8614–8621.
[28] X. Zhao, et al., Impedance studies on the capacity fading mechanism of Li(Ni0.5Co0.2Mn0.3)O2Cathode with high-voltage and high-temperature, J. Electrochem. Soc. 162 (2015) A2770–A2779, https://doi.org/10.1149/2.0851514jes.
[29] D. Aurbach, et al., The study of surface phenomena related to electrochemical lithium intercalation into Lix MO y host materials (M = Ni, Mn), J. Electrochem. Soc. 147 (2000) 1322–1331.
[30] K.M. Shaju, G.V.S. Rao, B.V.R. Chowdari, Performance of layered Li(Ni1/3Co1/3Mn1/3)O2 as cathode for Li-ion batteries, Electrochim. Acta 48 (2002) 145–151.
[31] Z. Wu, et al., Depolarized and fully active cathode based on Li(Ni0.5Co0.2Mn0.3)O2 embedded in carbon nanotube network for advanced batteries, Nano Lett. 14 (2014) 4700–4706, https://doi.org/10.1021/nl5018139.
[32] X. Zhang, et al., Aging of LiNi1/3Mn1/3Co1/3O2 cathode material upon exposure to H2O, J. Power Sources 196 (2011) 5102–5108, https://doi.org/10.1016/j.jpowsour.2011.02.009.
[33] A. Rougier, G.A. Nazri, C. Julien, Vibrational spectroscopy and electrochemical properties of LiNi0.7Co0.3O2 cathode material for rechargeable lithium batteries, Ionics 3 (1997) 170–176.
[34] C. Julien, L. El-Farh, S. Rangan, S. Massot, Studies of LiNi0.6Co0.4O2 cathode material prepared by the citric acid-assisted sol-gel method for lithium batteries, J. Sol. Gel Sci. Technol. 15 (1999) 63–72.
[35] Y. Bi, et al., Stability of Li2CO3 in cathode of lithium ion battery and its influence on electrochemical performance, RSC Adv. 6 (2016) 19233–19237, https://doi.org/10.1039/c6ra00648e.
[36] S.-K. Jung, et al., Understanding the degradation mechanisms of LiNi0.5Co0.2Mn0.3O2 cathode material in lithium ion batteries, Adv. Energy. Mater. 4 (2014), 1300787, https://doi.org/10.1002/aenm.201300787.